ANNALS OF GEOPHYSICS, 62, 6, DM673, 2019; doi: 10.4401/ag-7775

“DETERMINATION OF CODA WAVE ATTENUATION CHARACTERISTIC OF THE ARMUTLU PENINSULA AND ITS SURROUNDINGS (MIDDLE MARMARA REGION, TURKEY)”

Evrim Yavuz[*,1], Şerif Barış[1]

[(1)] Kocaeli University, Dept. of Geophysical Engineering, Umuttepe, 41380 Kocaeli, Turkey

Article history
Received May 28, 2018; accepted April 4, 2019.
Subject classification:
Armutlu Peninsula; Attenuation; Coda wave quality factor; Geothermal sources; North Anatolian Fault Zone.

ABSTRACT

The Armutlu Peninsula, is located in a geologically complex system on the North Anatolian Fault Zone and inside the high populated Marmara Region. Due to its location and importance, the Marmara Region has been subject to various studies in the past; now, this study is aimed to determine the local attenuation characteristic of the Armutlu Peninsula. In this study, 75 earthquake data that were recorded between 2013-2014, were analyzed by 9 seismic stations. The magnitudes (Ml) and the focal depths of the earthquakes vary from 1.5 to 3.3 and 0.9 to 16.9 km, respectively. A single back-scattering model was used for calculation of the coda wave quality factor. The lapse times were determined between 20 and 40 s at intervals of 5 s and they were filtered at central frequencies of 1.5, 3, 6, 9 and 12 Hz band-pass designed filter. Minimum 5 signal/noise ratio and 0.7 correlation coefficient data used to obtain reliable results. The CODAQ subroutine integrated in the SEISAN software was used for data processing. For each station, low values of the quality factor at 1 Hz (Q_o) and high values of the frequency dependent parameter (n) were determined. In the Armutlu Peninsula and its surroundings, $Q_c=51f^{0.91}$ for 20 s and $Q_c=112f^{0.72}$ for 40 s window lengths were calculated by using 9 stations. There is a tendency between increasing Q_o and decreasing n parameters. Otherwise, for station TRML, located near the geothermal hotspot, these parameters are in direct proportion with each other, as $Q_c=46f^{0.97}$ for 20 s and $Q_c=74f^{1.06}$ for 40 s window lengths. These parameter changes are directly connected with the geothermal activity.

1. INTRODUCTION

The Armutlu Peninsula is positioned in the high populated and industrialized Middle Marmara Region, between northern and middle branches of the North Anatolian Fault Zone (NAFZ), one of the active fault zones in Turkey. The expected large Istanbul earthquake have led to researches in and around the peninsula. Investigating the seismic wave attenuation is important in order to determine the medium structure of the region.

The energy of seismic waves decreases while propagating through the anelastic and heterogenic medium due to intrinsic attenuation, geometrical spreading and multipathing [Stein and Wysession, 2009]. The dimensionless quality factor-Q characterizes the decay rate of the seismic waves [Knopoff and MacDonald, 1958]. After the arrival of direct-*S* wave phase, the tail of a seismogram can be identified as coda wave generated by scattered waves within the lithosphere. The frequency dependent coda wave quality factor, Q_c, is a measure of

the rate of coda wave attenuation [Aki, 1969]. Local/regional recorded coda waves (up to 100 km epicentral distance) and their power spectra as well as coda duration are relatively independent from the focal distance [Aki and Chouet, 1975]. Q_c determination studies are generally performed in tectonically active fields, active volcanic regions, earthquake swarm areas, magmatic flows and geothermal areas [Del Pezzo et al., 2006; Mohamed et al., 2010; Dobrynina, 2011; Dasovi et al., 2013; Akinci et al., 2014; Akyol, 2015; Hasemi et al., 2015; Bachura and Fischer, 2016; Prudencio et al., 2017].

Focusing on the previous literature studies; on the Eastern Marmara region, $Q_c=115f^{0.90}$ was calculated for 25 s coda window length [Barış et al., 1992]. In and around Bursa (southern side of the Peninsula), Akyol et al. [2002] obtained $Q_s=46.59f^{0.67}$ with using accelerometers. $Q_c=(41\pm1.07)f^{(1.08\pm0.03)}$ was determined for a 50 s window length in the whole Marmara Region [Horasan et al., 1998]. On the Marmara Region, Kaşlılar-Özcan [1999] obtained $Q_c=(26\pm1.09)f^{(1.18\pm0.04)}$ for a 40 s window length. The studies of *S* wave attenuation in the whole Marmara Sea and the Middle-East Marmara Region provided $Q_s=(40\pm5)f^{(1.03\pm0.06)}$ and $Q_s=(54\pm18)f^{(1.05\pm0.19)}$, respectively [Horasan and Boztepe-Güney, 2004]. For the Adapazarı-Yalova line (in and western side of the Peninsula) and Marmara Sea-Saros Bay line (eastern side of the Peninsula), average $Q_c=(280\pm28)f^{(0.79\pm0.021)}$ and $Q_c=(252\pm26)f^{(0.81\pm0.022)}$ from 20, 30 and 40 s lapse times were derived, respectively [Sertcelik and Guleroglu, 2017]. Preliminary results of this study were obtained by Yavuz et al. [2016].

In this study, a detailed local coda wave quality factor determination for the Armutlu Peninsula and its vicinity was obtained for the first time.

2. TECTONIC AND GEOLOGICAL STRUCTURE OF THE ARMUTLU PENINSULA

The Marmara Region, which has the highest population density and industrialization in the country, is located in northwestern Turkey. The Armutlu Peninsula is in the central part of the Marmara Region and it still continues to receive migration from other cities.

The dextral NAFZ is one of the significant fault system in Turkey. The tectonic structure of Armutlu Peninsula is controlled by the western realm of this fault zone. 24±1 mm/yr movement of the main fault system and its strands generate the crackled inner-structure and complex crustal regime [Reilinger et al., 1997, 2006; McClusky et al., 2003]. This feature produces micro-seismic events in and around the peninsula (Figure 1).

The August 17, 1999 Kocaeli (Mw=7.4) and the November 12, 1999 Düzce (Mw=7.2) earthquakes occurred very close to the eastern part of the peninsula and they disastrously affected east and middle parts of the Marmara Region [Erdik, 2001]. After these large right lateral strike-slip mechanism earthquakes, some moderate shakes (the 2016 Gemlik earthquake – Mw=5.2 is the largest one) were recorded on the peninsula and influenced the local people. A major earthquake has not been recorded in the last century along the southern segment of the peninsula [Caka, 2012].

The Armutlu Peninsula which is located between two branches of NAFZ, consists of Lower Paleozoic-Upper Cretaceous metamorphic rocks and Paleozoic aged slightly metamorphosed rocks as basement. Those rocks are overlaid by Upper Cretaceous-Eocene volcanic and sedimentary rocks. A granite emplacement occurred in Middle Eocene and from Miocene to present day aged sedimentary rocks covers the whole northern part of the peninsula [Yilmaz et al., 1995].

The geothermal activity is presumedly under controlled by NAFZ and geothermal sources are widely spread over the peninsula. The hottest point, Termal, is located on the northern realm of the peninsula and its average temperature is 60-70°C; otherwise along the southern part, the thermal regions have 20-30°C water temperature [Eisenlohr, 1997] (Figure 1). The seismic activity of the region is associated with both fault systems and the geothermal activity. E.g. in 2014, the Termal geothermal reservoir caused a seismic swarm [KOERI press release, 2015; Yavuz et al., 2015].

3. METHOD

Coda waves that are generated by local earthquakes can be interpreted as backscattered *S* waves from the heterogeneities of Earth's crust and upper mantle. Aki and Chouet [1975] developed the theory of the single backscattering model and in this study this model was used for estimation of coda wave quality factor (Q_c). The coda wave amplitude decay can be defined as a function of time, t, and frequency, f, as

$$A(f,t)=c(f)t^{-\alpha}\exp(-\pi ft/Q_c) \quad (1)$$

where A(f,t) is the coda wave amplitude filtered at a specific central frequency (f); t is the lapse time, Q_c is the coda wave quality factor, c is the source function at frequency (f) and α is the geometrical spreading factor that is here chosen equal to 1 for body waves [Sato and Fehler, 1998]. Considering α=1 and taking a logarithm of Equation 1, we obtain

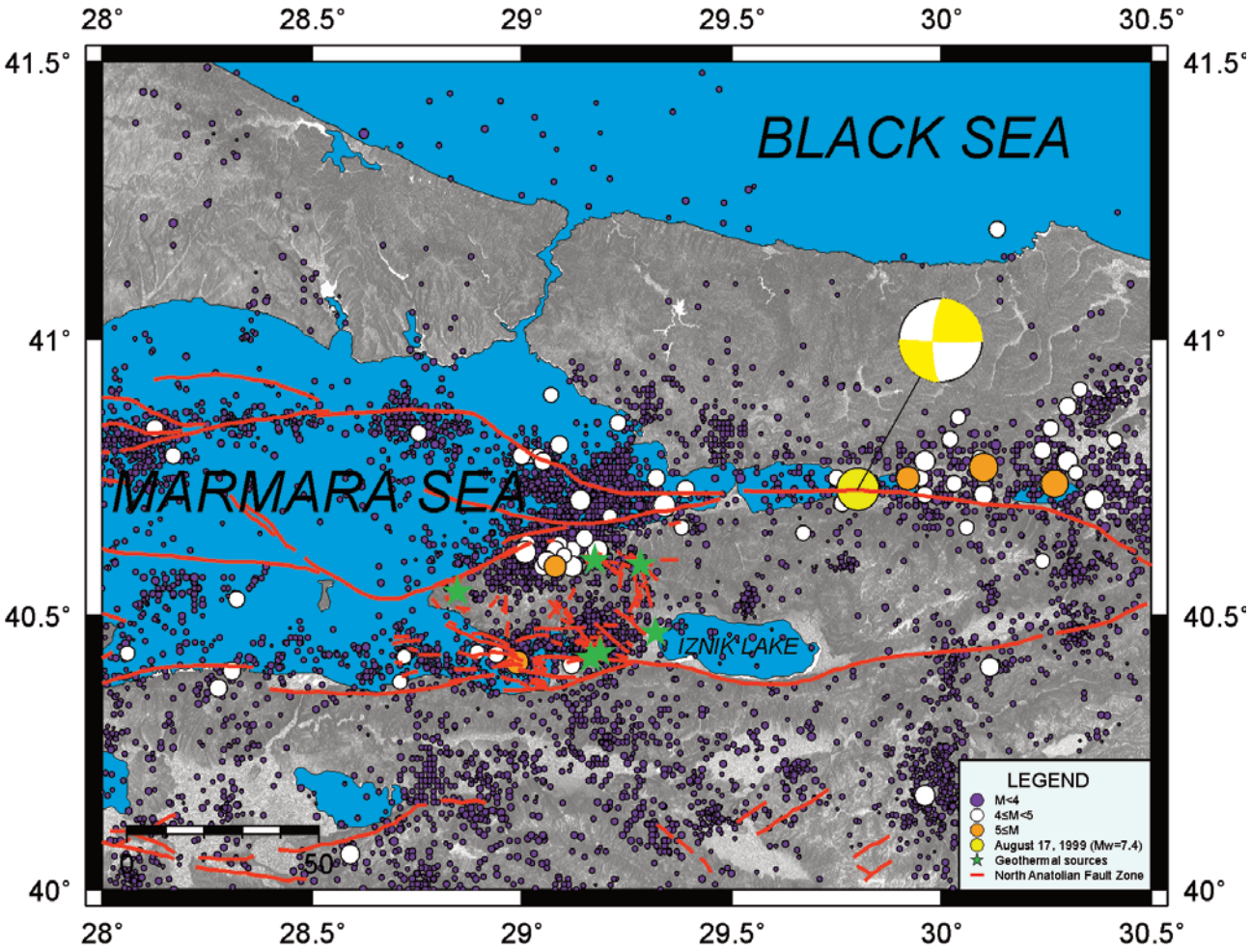

FIGURE 1. The tectonic features of the middle and eastern Marmara Region and its seismic activity in last two decades. Red lines indicate the North Anatolian Fault Zone, its branches and the micro–fractures [Eisenlohr 1997; Kuşçu et al. 2009; Pınar et al. 2003; Caka 2012].

$$\ln[A(f,t)]=\ln c(f) - \ln(t) - \pi f t/Q_c(f) \quad (2)$$

Regarding the ray paths that propagate from each scattered heterogeneity, the frequency dependent coda wave quality factor can be calculated from the slope $\pi f/Q_c$

The general dependence of Q_c on f can be described as

$$Q_c(f)=Q_o[f/f_o]^n \quad (3)$$

where, Q_o is the value of Q_c at 1 Hz, f_o is the reference frequency, here assumed as 1 Hz and n is the frequency dependence parameter. The Q_o and n values represent the general geological structure of the region. Low values of Q_o (<200) characterize the region with high tectonic activity; otherwise, high values of Q_o (>600) describe stable seismic activity [Aki and Chouet, 1975; Mak et al., 2004; Sertçelik, 2012]. At the same time, if n is higher than 0.8, the crust and upper mantle are tectonically active; while n values lower than 0.5, characterize an inactive region [Atkinson, 2004; Dasovic et al., 2012; Ranasinghe et al., 2014; Dobrynina et al., 2017; Banerjee and Kumar, 2017].

4. DATA AND PROCESS

The ARmutlu NETwork (ARNET) was installed at the end of 2005 with currently 27 active seismic stations operating by Kocaeli University Earth and Space Sciences Research Center and Helmholtz-Zentrum Potsdam DeutschesGeo-ForschungsZentrum (GFZ) [Tunç et al., 2011]. To determine attenuation features, 75 earthquake data recorded by 9 ARNET three components seismic stations (Table 1) between 2013-2014 are used (Figure 2). The sampling rate for all stations is set as 100 samples per second. The local magnitude range of the events is from 1.5 to 3.3 and the depths are between 0.9-16.9 km (Appendix 1). The events

Station code	Station Location	Sensor and type	Latitude (°N)	Longitude (°E)	Elevation (m)
ALTN	Altintas/Bursa	CMG-40T / BB	40.35783	28.96383	30
AVDN	Avdancik/Bursa	CMG-40T / BB	40.29327	29.16459	476
DLMC	Delmece/Yalova	L-4C / SP	40.56256	29.00388	728
HYDR	Haydariye/Bursa	L-4C / SP	40.51317	29.12700	390
KRSK	Karsak/Bursa	CMG-3TDE / BB	40.40500	29.25817	170
SDSN	Sudusen/Yalova	L-4C / SP	40.57531	29.14996	204
SLMY	Selimiye/Yalova	CMG-3TDE / BB	40.51757	28.98584	460
TRML	Termal/Yalova	L-4C / SP	40.60950	29.17350	204
TSVK	Tesvikiye/Yalova	CMG-40T / BB	40.62667	29.08733	70

TABLE 1. The information of seismic stations of ARNET that are used for coda wave attenuation analysis. Abbreviations; BB: broadband, SP: short-period.

are located within 0.6-75.6 km epicentral distances; however, the majority of the distances distributes within 40 km.

The first locations of the earthquakes were determined by using the SEISAN software [Havskov and Ottemoller, 1999] with the HYPOCENTER algorithm. To this aim, all ARNET stations and the Özalaybey et al. [2002] 1-D velocity model are used (Table 2). Minimum five azimuthally well-distributed stations and up to 0.5 root mean square (RMS) values are the criteria used for obtaining first locations.

Higher than 5 signal-to-noise ratio (S/N) of the seismograms allow us to obtain reasonable Q_c calculations [Ottemoller et al., 2014]. The elimination of direct *S*-wave phases is important to determine the beginning of the coda wave [Rautian and Khalturin, 1978]. The start of the coda (t_{start}) as measured from the origin time should be placed at 1.5, 2 or 2.5 time the *S*-wave travel time (t_s) [Havskov et al., 1989]. It is called the lapse time. $2t_s$ is generally acceptable for local earthquakes [Spudich and Bostwick, 1987; Mukhopadhyay et al., 2010] and we decided to assume $t_{start} = 2t_s$ for all seismograms analyzed in the present study. Minimum 20 s coda window length is acceptable while larger windows could be served for more stabilized solutions [Gupta et al., 2012; Ottemoller et al., 2014]. According to the epicentral distances and magnitude of earthquakes, we have tried longer window lengths with 5 s step increases, but smaller than 40 s in order to analyze a sufficient number of data with ≥5 S/N ratio [Ottemoller et al., 2014; personal communication with Lars Ottemoller, 2015].

The overall variation of the Q_c in different frequencies is an important indication of the heterogeneity of the medium [Calvet and Margerin, 2013]. All coda records were band-pass filtered with 1.5, 3, 6, 9, 12 Hz central frequencies. The bandwidth of each central frequency f_c is crucial to get an equal amount of energy. All designed filters should have the same value $(f_h\text{-}f_l)/f_c$; where f_h and f_l are the high corner and low corner frequencies, respectively [Aki and Richards, 2002; Ottemoller et al., 2014]. The filters are designed with the following central frequency (corresponding bandwidth) values: 1.5 Hz (1-2), 3 Hz (2-4), 6 Hz (4-8), 9 Hz (6-12) and 12 Hz (8-16). The purpose of using a central frequency as 1.5 Hz is to prevent the loss of long-period waves that can be recorded at distant stations; but, 12 Hz is also required to consider short-period waves that will be seen in the stations at close epicentral distances.

In order to calculate the quality factor, the CODAQ subroutine contained in the SEISAN software package was used [Havskov and Ottemoller, 1999]. Both the three components recorded at each station and their average were chosen for Q_c calculation, assuming a minimum correlation coefficient of 0.7 [personal communication with Lars Ottemoller, 2015]. As an example, in Figure 3, the coda wave analysis obtained from the SEISAN software for a vertical component at station AVDN is shown.

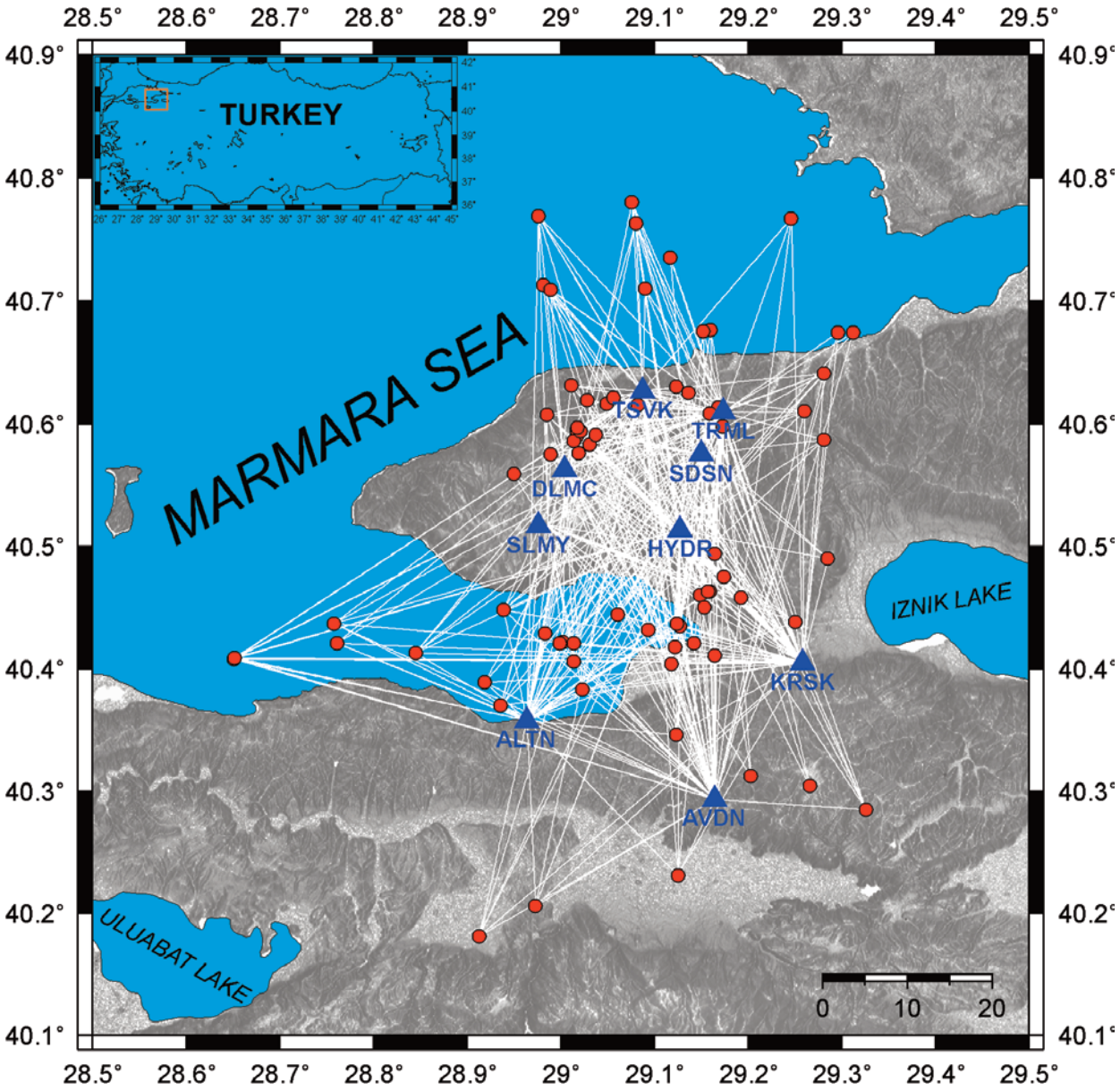

FIGURE 2. Map of the studied area. Red circles and blue triangles depict the epicenters of the earthquakes and seismic stations, respectively. White lines are the minimum–distance paths between epicenter and seismic station that are recorded. The orange rectangle indicates the study area.

Depth (km)	Vp (km/s)	Vs (km/s)
0.0	2.90	1.68
1.0	5.70	3.29
6.0	6.10	3.53
20.0	6.80	3.93
33.0	8.05	4.65

TABLE 2. 1-D velocity model for locating earthquakes in the study area [Özalaybey et al. 2002].

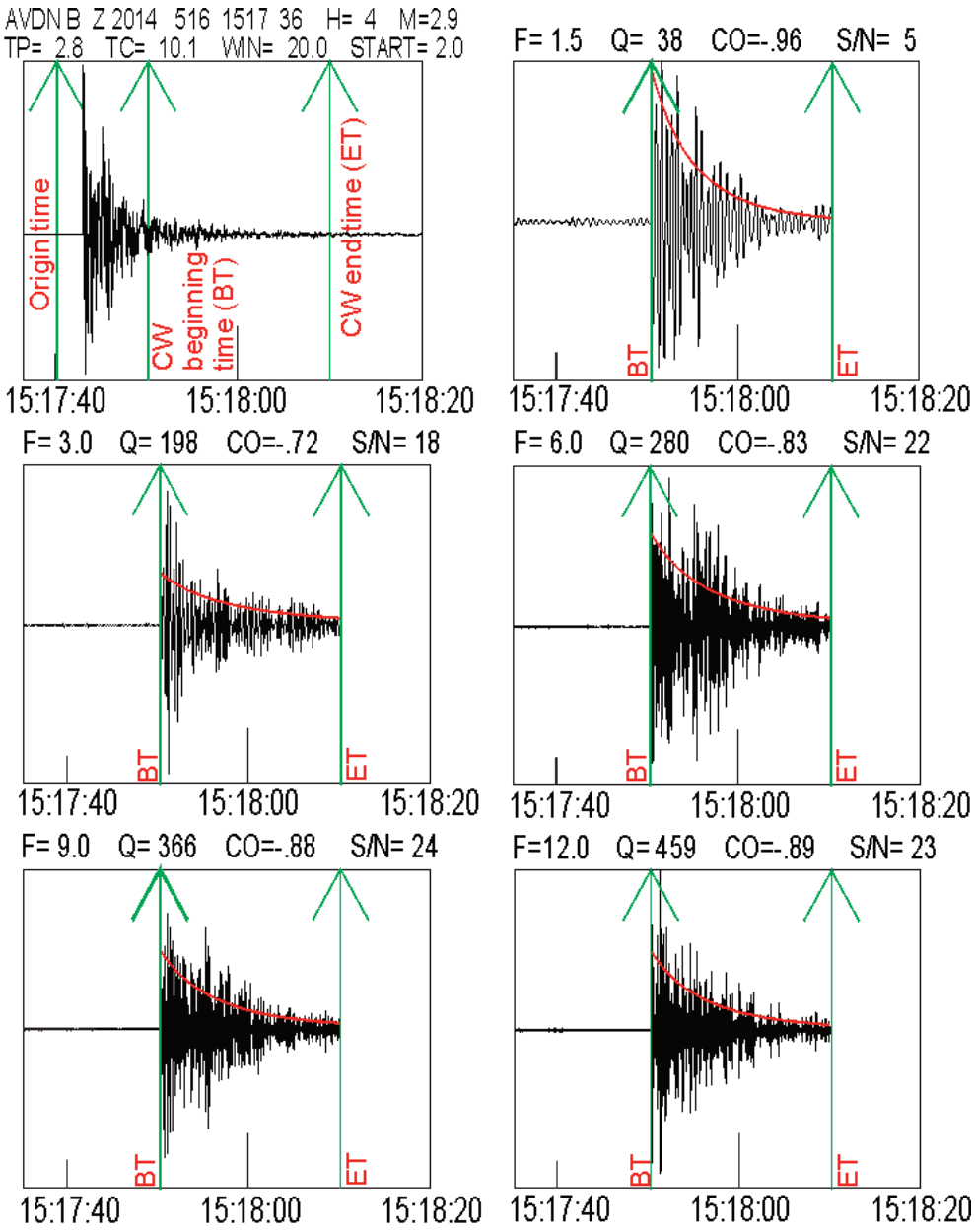

FIGURE 3. Example of coda wave analysis with different central frequencies on the vertical (Z) component of station AVDN for the 16.05.2014 15:17:40 earthquake. The red curves indicate the coda wave decay slopes. Abbreviations; H: focal depth (km), M: magnitude (Ml), TP: P wave travel time, TC: start time of coda window relative to origin time, WIN: coda window length (s), START: start time in coda window in terms of S travel times, F: central frequency (Hz), Q: average quality factor, CO: correlation coefficient and S/N: signal/noise ratio. The origin time, the beginning and the end of the coda window are marked by green arrows.

5. RESULTS AND DISCUSSION

In the computation of the quality factor for the investigated area, the stations' location and the distributions of the earthquakes are important parameters. These parameters refer to the ray path, followed by the earthquake waves that depend on the physical structure of the crust through which they travel and the energy loss due to friction, porosity, fluid content, etc. [Barton, 2007].

Q_o and n values at different time window lengths for each station were determined (Table 3). The Q_c values variation with different lapse time windows and frequencies was calculated for each stations and also all stations together (Figure 4).

Each station exhibits relatively low values of quality factor (Q) and high n values. These values are comparable to the ones evaluated in other regions with high tectonic activity such as Aswan Reservoir area Egypt [Mohamed et al.,

Window Length (s)	ALTN			AVDN			DLMC		
	$Q_0 \pm \sigma$	$n \pm \sigma$	N	$Q_0 \pm \sigma$	$n \pm \sigma$	N	$Q_0 \pm \sigma$	$n \pm \sigma$	N
20	54±5	0.94±0.04	237	54±8	0.90±0.06	327	55±2	0.85±0.02	242
25	68±8	0.89±0.06	204	64±9	0.86±0.06	255	67±3	0.78±0.02	207
30	95±9	0.79±0.05	168	79±12	0.81±0.07	199	88±5	0.71±0.03	172
35	112±8	0.74±0.04	137	89±12	0.79±0.07	143	104±8	0.68±0.04	147
40	126±18	0.75±0.07	105	119±22	0.70±0.09	105	129±22	0.63±0.08	116
Window Length (s)	HYDR			KRSK			SDSN		
	$Q_0 \pm \sigma$	$n \pm \sigma$	N	$Q_0 \pm \sigma$	$n \pm \sigma$	N	$Q_0 \pm \sigma$	$n \pm \sigma$	N
20	47±2	0.96±0.02	358	53±8	0.89±0.07	319	46±6	0.91±0.06	157
25	53±5	0.91±0.04	315	69±9	0.83±0.06	243	52±9	0.89±0.07	137
30	64±6	0.85±0.04	269	79±16	0.80±0.09	195	79±9	0.74±0.05	109
35	81±10	0.80±0.06	225	92±23	0.78±0.11	130	100±15	0.69±0.07	97
40	101±9	0.74±0.04	177	111±29	0.75±0.12	98	123±21	0.65±0.08	62
Window Length (s)	SLMY			TRML			TSVK		
	$Q_0 \pm \sigma$	$n \pm \sigma$	N	$Q_0 \pm \sigma$	$n \pm \sigma$	N	$Q_0 \pm \sigma$	$n \pm \sigma$	N
20	64±5	0.82±0.04	196	46±3	0.97±0.04	137	48±8	0.94±0.07	181
25	74±9	0.76±0.06	165	51±3	1.03±0.04	123	62±6	0.88±0.05	131
30	86±12	0.74±0.06	138	61±6	1.03±0.06	90	70±8	0.87±0.05	85
35	106±11	0.69±0.05	129	71±6	1.02±0.06	64	79±11	0.84±0.07	48
40	110±9	0.67±0.04	110	74±6	1.06±0.05	45	118±9	0.70±0.04	37

TABLE 3. The Q_0 and n values variation with different time window lengths for each station. Abbreviations; N: number of data, **σ**: standard deviation.

2010], Saurashtra Region Gujarat (India) [Sharma et al., 2012], Kumaun Himalaya [Singh et al., 2012], Baikal Rift System [Dobrynina et al., 2016], Northwestern Himalayan (India) Region [Kumar et al., 2016], Northern Morocco [Boulanouar et al., 2018]. Then our results suggest that the Armutlu Peninsula has high tectonic and seismic activity.

The stations ALTN, AVDN and KRSK are located in the southern side of the peninsula, northern part of Bursa and so close to the middle and southern branch of the North Anatolian Fault Zone. Hence the Q_0 and n values are conformable with each other due to the fact that the coda waves arriving at very close stations spread from similar scatters in the region. The low Q_0 values could indicate the plate movements on the NAFZ.

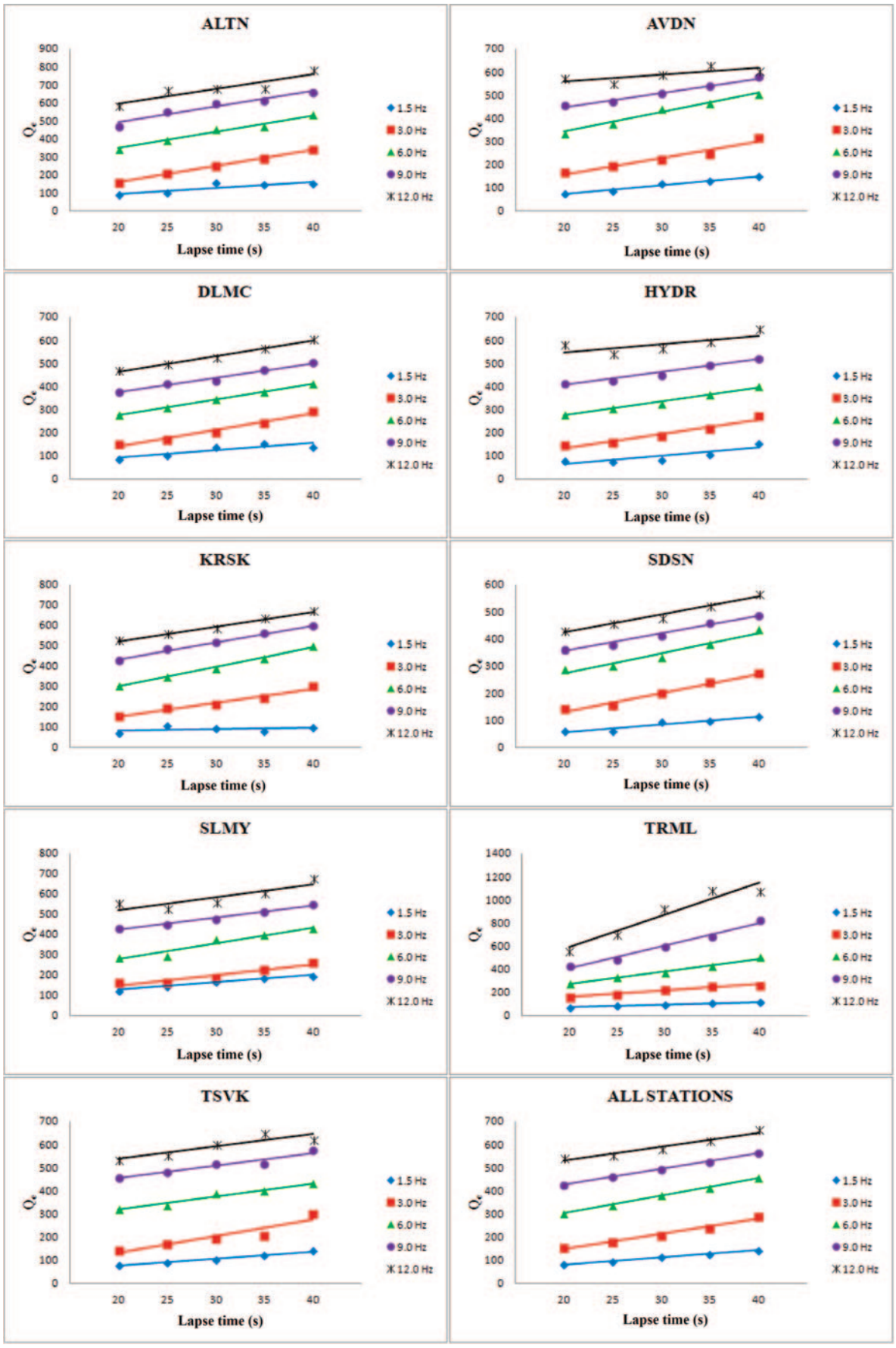

FIGURE 4. The Q_c values alteration with increasing lapse time windows and different central frequencies for each station and all stations together.

Window Length (s)	1.5 Hz (1-2) $Q_c \pm \sigma$	N	3 Hz (2-4) $Q_c \pm \sigma$	N	6 Hz (4-8) $Q_c \pm \sigma$	N	9 Hz (6-12) $Q_c \pm \sigma$	N	12 Hz (8-16) $Q_c \pm \sigma$	N
20	83±40	146	153±55	358	302±97	458	427±132	449	540±171	425
25	94±45	116	178±69	313	336±115	403	461±154	403	553±164	352
30	115±55	85	208±83	268	382±132	370	493±143	329	580±152	267
35	128±63	59	240±86	241	412±115	319	527±143	264	615±149	187
40	141±62	43	288±97	199	454±124	254	563±143	210	662±165	123

TABLE 4. The Q_c values alteration with lapse times and different central frequencies with using all stations. Abbreviations; N: number of data, σ: standard deviation.

The stations located inside the peninsula, except the station TRML, reveal a proportional trend between Q_0 and lapse times. These values suggest the region is dominated by local faults and fractures due to the connectivity between the north and middle branches of the NAFZ. For instance, in the Kopili Fault Zone (India), the coda Q study performed by Bora et al. [2018] demonstrates that the seismic activity is in correlation with the low values of coda wave decay. Additionally, in NW Himalayan Region, Kumar et al. [2005] evaluated low Q_0 values through the whole main boundary thrusts and other fault segments.

The Termal district of Yalova, which has a geothermal spot inside the peninsula, houses the station TRML that works very close to this source. The obtained Q_0 values of station TRML are lower in comparison with the other stations. According to the 20 to 40 s time windows, the Q_0 values are increasing from 46 to 74 and the n values are also rising from 0.97 to 1.06. Naghavi et al. [2017] obtained high attenuation for the region with thermal springs and volcanic structure in North West of Iranian plateau. Canas et al. [1995] found low Q_0 values near the Canary Islands that have high magmatic activity.

Seismic waves attenuate due to the scatters caused by heterogeneities or an intrinsic phenomenon attributed to the anelastic behavior of the medium through which they propagate. Intrinsic attenuation is very sensitive to the physical condition of the underlying medium, while scattering attenuation indicates the degree of heterogeneity [Dainty, 1981; Sato and Sacks, 1989]. The scattering characteristic could express heterogeneities of the NAFZ and micro-fractures; otherwise, the intrinsic effect may be the dominant one for a geothermal region.

After determining the individual quality factor for each station, a single calculation was performed for all stations. It identifies an average attenuation characteristic for the Armutlu Peninsula and its vicinity. The number of high-quality data is low on long-periodic waves, such as 1.5 Hz central frequency, and increasing lapse times owing to the localized area of study. Hence, more reliable and useful results could be obtained from lower lapse times and higher frequency content data. These two parameters affect the standard deviation value directly (Table 4).

From Table 5 results the coda wave attenuation can be estimated as $Q_c=(51\pm4)f^{(0.91\pm0.04)}$ for 20 s lapse time through 2154 number of data. This function could be identified as the general attenuation law of the Armutlu Peninsula and its surroundings. Also, it is in a correlation with individual quality factor calculations for each station.

Window Length (s)	All Stations		
	$Q_0 \pm \sigma$	$n \pm \sigma$	N
20	51±4	0.91±0.04	2154
25	62±5	0.86±0.04	1170
30	77±7	0.80±0.04	1425
35	92±9	0.76±0.05	1120
40	112±13	0.72±0.06	855

TABLE 5. The Q_0 and n values variation for all stations together. Abbreviations; N: number of data, σ: standard deviation.

Window Length (s)	$Q_0 \pm \sigma$	$n \pm \sigma$	Area	Reference
25	115	0.90	Eastern Marmara Region	Barış et al. (1992)
-	$Q_S=46.59f^{0.97}$		Bursa	Akyol et al. (2002)
50	41±1.07	1.08±0.03	Marmara Region	Horasan et al. (1998)
40	26±1.09	1.18±0.04	Marmara Region	Kaşlılar-Özcan (1999)
-	$Q_S=40\pm5f^{(1.03\pm0.06)}$		Marmara Sea	Horasan and Boztepe-Güney (2004)
-	$Q_S=54\pm18f^{(1.05\pm0.19)}$		Middle-East Marmara Region	Horasan and Boztepe-Güney (2004)
20-40	280±28	0.79±0.021	Adapazarı-Yalova line	Sertcelik and Guleroglu (2017)
20-40	252±26	0.81±0.022	Marmara Sea-Saros Bay line	Sertcelik and Guleroglu (2017)
<60	65±5	1.05±0.04	Dead Sea Region	Eck (1988)
10-20	33	1.01	Northern Greece	Hatzidimitriou (1993)
30	101±6	0.94±0.11	East Central Iran	Ma'hood and Hamzehloo (2009)
25	121±55	0.97±0.26	Southwestern Iran	Rahimi and Hamzehloo (2008)
-	79±2	1.07±0.08	Central Iran	Rahimi et al. (2010)
-	126	1.05	Israel	Meirova and Pinsky (2004)
20	51±4	0.91±0.04	Armutlu Peninsula	This study

TABLE 6. Q studies in the Marmara Region and the neighbors of Turkey.

The attenuation rate difference between eastern and western side of the peninsula attracts the attention (Table 3). Each side is exposed to a different extension regime. It is known that both thermal sources and local fractures are dominant in the west [personal communication with A.M. Celal Şengör, 2018]. The sharp variation of Q_0 values is interpreted as the result of different inner structures which diversify according to the rarity of local micro-fractures and faults at the eastern side, on the contrary of the western side. According to increasing time window lengths, it is determined that the inner structures of the regions, except for the thermal area, resembles each other. We can interpret these results considering that structural deformation is dominant near the surface because of the local faults, while it is reduced as well as medium heterogeneity at larger depth.

Among the earlier studies on the neighboring areas of Turkey, Eck [1988] found $Q_0=65\pm5$ and n=1.05±0.04 for up to 60 s lapse time in Dead Sea Region around Israel; Hatzidimitriou [1993] calculated Q_0 and n values as 33 and 1.01, respectively for 10 to 20 s lapse time windows in Northern Greece; Ma'hood and Hamzehloo [2009] obtained $Q_c=(101\pm6)f^{(0.94\pm0.11)}$ for 30 s in East Central Iran; before and after 2006 Darb-e Astane Earthquake (M=6.1) that located in Southwestern Iran, $Q_c=(121\pm55)f^{(0.97\pm0.26)}$ for aftershocks and $Q_c=(144\pm24)f^{(0.42\pm0.23)}$ for foreshocks

at 25 s were calculated by Rahimi and Hamzehloo [2008]; the average frequency relation for Central Iran was determined as $Q_c=(79\pm2)f^{(1.07\pm0.08)}$ by Rahimi et al. [2010]; a regional $Q_c=126f^{1.05}$ relation was approximated by Meirova and Pinsky [2004] based on S wave coda decay rate for Israel.

The discrepancies between the present results and those ones obtained in previous studies of Marmara Region reported in "Introduction" section and in Table 6 might be due to the differences in the considered window lengths and kind of quality factor vary from one author to another [Barış et al., 1992; Horasan et al., 1998; Kaşlılar-Özcan, 1999; Akyol et al., 2002; Horasan and Boztepe-Güney, 2004; Sertcelik and Guleroglu, 2017]. Generally, most of the studies demonstrate <200 of Q values and this suggest an active tectonic settings.

6. CONCLUSION

In and around the Armutlu Peninsula, nine seismic stations from the ARmutlu NETwork (ARNET) were used to estimate the quality factor (Q) through a single back-scattering model with 75 earthquake data that were recorded between 2013-2014. The values of Q_o and n expressing the frequency dependence of the quality factor vary from 51 to 112 and 0.91 to 0.72 for 20 and 40 s lapse times, respectively. These variations indicate a highly complex and tectonically active medium in agreement with the presence of the NAFZ and widespread micro-fractures in the study. In this localized area, the general coda wave quality factor relation results as $Q_c=(51\pm4)f^{(0.91\pm0.04)}$ for 20 s lapse time. This function is indicative of the general attenuation characteristic of the region.

The geothermal activity around the station TRML is remarkably recognized in this study. The Q_o and n values vary from 46 to 74 and 0.97 to 1.06 for 20 and 40 s lapse times, respectively. The direct proportion of Q_o and n values is in agreement with the presence of thermal springs and thermal fluidity even depth.

The quality factor results obtained in this study suggest dominant and active tectonics for the region in agreement with the presence of the NAFZ, local fractures and thermal sources.

Acknowledgements. This study derives from the MSc. thesis of the first author (EY). The authors give many thanks to Dr. Deniz Çaka for recommendations and contributions. The data used in this study were recorded by the ARmutlu NETwork (ARNET); therefore, we are grateful to both Kocaeli University and GFZ collaboration colleagues for sharing the data. We would like to thank Prof. Maria Elina Belardinelli (sector editor) and anonymous reviewers for their crucial and helpful comments.

REFERENCES

Aki, K. (1969). Analysis of the seismic coda of local earthquakes as scattered waves, J. Geophys. Res., 74(2), 615-631.

Aki, K., B. Chouet, (1975). Origin of coda waves: source, attenuation and scattering effects, J. Geophys. Res., 80, 3322-3342.

Aki, K., P. G. Richards, (2002). Quantitative seismology; theory and methods, W. H. Freeman, San Francisco.

Akinci, A., L. Malagnini, R. B., Herrmann, D. Kalafat, (2014). High-Frequency Attenuation in the Lake Van Region, Eastern Turkey, Bull. Seis. Soc. Am., 104(3); 1400-1409.

Akyol, N. (2015). Lapse time dependence of coda wave attenuation in Central West Turkey. Tectonophysics, 659, 53-62.

Akyol, N., A. Akinci, H. Eyidogan (2002). Seperation of Source, Propogation and Site Effects from S Waves of Local Earthquakes in Bursa Region, Northwestern Turkey, Pure Appl. Geophys., 159, 1253-1269.

Atkinson, G.M. (2004). Empirical Attenuation of Ground-Motion Spectral Amplitudes in Southeastern Canada and the Northeastern United States, Bull. Seis. Soc. Am., 94, 1079-1095.

Bachura, M., T. Fischer (2016). Coda attenuation analysis in the West Bohemia/Vogtland earthquake swarm area, Pure Appl. Geophys., 173(2), 425-437.

Banerjee, S., A. Kumar (2017). Determination of Seismic Wave Attenuation for the Garhwal Himalayas, India. Geosci. Res., 2(2), 105-126.

Barış Ş., A. Pınar, C. Gürbüz, S. B. Üçer, K. Nishigami (1992). The Coda Q estimation and its spatial distribution in the western part of the North Anatolian Fault Zone, Turkey, Boğaziçi University Press, 501, 43-60.

Barton, N. (2007). Rock quality, seismic velocity, attenuation and anisotropy, Taylor&Francis, London.

Bora, N., R. Biswas, A. A. Dobrynina, (2018). Regional variation of coda Q in Kopili fault zone of northeast India and its implications, Tectonophysics, 722, 235-248.

Boulanouar, A., L. El Moudnib, S. Padhy, M. Harnafi, A. Villasenor, J. Gallart, A. Pazos, A. Rahmouni, M. Boukalouch, J. Sebbani, (2018). Estimation of coda wave attenuation in Northern Morocco, Pure Appl.

Geophys., 175(3), 883-897.

Caka, D. (2012). Shear-wave splitting analysis in and around Armutlu Peninsula, PhD. dissertation, Kocaeli University, Kocaeli (in Turkish).

Calvet, M., L. Margerin (2013). Lapse-time dependence of coda Q: Anisotropic multiple-scattering models and application to the Pyrenees., Bull. Seis. Soc. Am., 103(3), 1993-2010.

Canas, J. A., L. G. Pujades, M. J. Blanco, V. Soler, J. C. Carracedo (1995). Coda-Q distribution in the Canary Islands, Tectonophysics, 246, 245-261.

Dainty, A. M. (1981). A scattering model to explain seismic Q observations in the lithosphere between 1 and 30 Hz, Geophys. Res. Let., 8(11), 1126-1128.

Dasović, I., M. Herak, D. Herak (2012). Attenuation of coda waves in the contact zone between the Dinarides and the Adriatic Microplate, Stud. Geophys. Geod., 56(1), 231-247.

Dasović, I., M. Herak, D. Herak (2013). Coda-Q and its lapse time dependence analysis in the interaction zone of the Dinarides, the Alps and the Pannonian basin, Phys. Chem. Earth, Parts A/B/C 63, 47-54.

Del Pezzo, E., F. Bianco, L. De Siena, A. Zollo (2006). Small scale shallow attenuation structure at Mt. Vesuvius, Italy, Phys. Earth Planet. Inter., 157(3-4), 257-268.

Dobrynina, A. A. (2011). Coda-wave attenuation in the Baikal rift system lithosphere, Phys. Earth Planet. Inter., 188.1, 121-126.

Dobrynina, A. A., J. Albaric, A. Deschamps, J. Perrot, R. W. Ferdinand, J. Deverchere, V. A., San'kov, V. V. Chechel'nitskii (2017). Seismic wave attenuation in the lithosphere of the North Tanzanian divergence zone (East African rift system), Russ. Geol. Geophys., 58(2), 253-265.

Dobrynina, A. A., V. A. Sankov, V. V Chechelnitsk, J. Deverchere (2016). Spatial changes of seismic attenuation and multiscale geological heterogeneity in the Baikal rift and surroundings from analysis of coda waves, Tectonophysics, 675, 50-68.

Eck, T. V. (1988). Attenuation of coda waves in Dead Sea Region, Bull. Seismol. Soc. Am., 78(2), 770-779.

Eisenlohr, T. (1997). The thermal springs of the Armutlu Peninsula (NW Turkey) and their relocationship geology and tectonic, Active Tectonics of Northwestern Anatolia-The Marmara Poly-project, ETH-Zurich, 197-228.

Erdik, M. (2001). Report on 1999 Kocaeli and Duzce (Turkey) Earthquakes, Structural control for Civil and Infrastructure Engineering: World Scientific, 149-186.

Gupta, A. K., A. K. Sutar, S. Chopra, S. Kumar, B. Rastogi (2012). Attenuation characteristics of coda waves in Mainland Gujarad (India), Tectonophysics, 530, 264-271

Hasemi, A., H. Miura, M. Ishizawa, M. Kosuga, N. Umino, N., A. Hasegawa (2015). Crustal structure in and around the Onikobe geothermal area, northeastern Honshu, Japan, inferred from the spatial variation of coda decay, Phys. Earth Planet. Inter., 244, 23-31.

Hatzidimitriou, P. M. (1993). Attenuation of coda waves in Northern Greece, Pure Appl. Geophys., 140(1), 63-78.

Havskov J., S. Malone, D. McClury, R. Crosson (1989). Coda-Q for the state of Washington, Bull. Seis. Soc. Am., 79, 1024-1038.

Havskov J., L. Ottemöller (1999). SeisAn Earthquake analysis software, Seis. Res. Lett., 70, 532-534.

Horasan G., A. Kaşlılar-Özcan, A. Boztepe-Güney, N. Türkelli (1998). S-wave attenuation in the Marmara Region, northwestern Turkey, Geophys. Res. Lett., 25, 2733-2736.

Horasan G., A. Boztepe-Güney (2004). S-wave attenuation in the Sea of Marmara, Turkey, Phys. Earth Planet. Inter., 142, 215-224.

Kaşlılar-Özcan A., (1999). Investigation of attenuation structure in the Marmara region, PhD. dissertation, Istanbul Technical University, Istanbul (in Turkish).

Knopoff, L., G. F. J. MacDonald (1958). Attenuation of small amplitude stress waves in solids, Rev. Mod. Phys., 30(4), 1178.

KOERI, Kandili Observatory and Earthquake Research Institute (2014) 2-4 Ağustos 2014 Termal-Yalova Deprem Etkinliği, press release (in Turkish).

Kumar, N., I. A. Parvez, H. S. Virk (2005). Estimation of coda wave attenuation for NW Himalayan region using local earthquakes, Phys. Earth Planet. Inter., 151, 243-258.

Kumar, S., P. Singh, P. Singh, S. Biswal, M. P. Parija (2016). Frequency dependent attenuation characteristics of coda waves in the Northwestern Himalayan (India) region, J. Asian Earth Sci., 117, 337-345.

Kuşçu, I., M. Okamura, H. Matsuoka, K. Yamamori, Y. Awata, S. Özalp (2009). Recognition of active faults and step over geometry in Gemlik bay, Sea of Marmara, NW Turkey, Marine Geol., 260, 90-101.

Ma'hood, M., H. Hamzehloo (2009). Estimation of coda wave attenuation in East Central Iran, J. Seismol., 13(1), 125-139.

Mak, S., L. S. Chan, A. M Chandler, R. C. H. Koo (2004). Coda Q estimates in the Hong Kong region, J. Asian Earth Sci., 24, 127–136.

McClusky, S., R. Reilinger, S. Mahmoud, D. B. Sari, A. Tealeb (2003). GPS constraints on Africa (Nubia)

and Arabia plate motions, Geophys J. Int., 155, 126-138.

Meirova, T., V. Pinsky (2014). Seismic wave attenuation in Israel region estimated from the multiple lapse time window analysis and S-wave coda decay rate, Geophys. J. Int., 197, 581-590.

Mohamed, H. H., S. Mukhopadhyay, J. Sharma (2010). Attenuation of coda waves in the Aswan Reservoir area, Egypt, Tectonophysics, 492(1), 88-98.

Mukhopadhyay, S., J. Sharma, E. Del-Pezzo, N. Kumar (2010). Study of attenuation mechanism for Garwhal–Kumaun Himalayas from analysis of coda of local earthquakes, Phys. Earth Planet. Inter., 180(1), 7-15.

Naghavi, M., H. Rahimi, A. Moradi, S. Mukhopadhyay (2017). Spatial variations of seismic attenuation in the North West of Iranian plateau from analysis of coda waves, Tectonophysics, 708, 70-80.

Ottemoller, L., P. Voss, J. Havskov (2014). SEISAN Earthquake Analysis Software for Windows, Linux, Solaris and MACOSX.

Özalaybey, S., M. Ergin, M. Aktar, C. Tapırdamaz, F. Biçmen, A. Yörük (2002). The 1999 İzmit Earthquake Sequence in Turkey: Seismological and Tectonic Aspects, Bull. Seis. Soc. Am., 92, 376-386.

Pınar, A., Kuge, K., Honkura, Y. (2003). Moment tensor inversion of recent small to moderate sized earthquakes: implications for seismic hazard and active tectonics beneath the Sea of Marmara, Geophys. J. Int., 153, 133-145.

Prudencio, J., Aoki, Y., Takeo, M., Ibanez, J. N., Del Pezzo, E., Song, W. Z. (2017). Seperation of scattering and intrinsic attenuation at Asama volcano (Japan): Evidence of high volcanic structural contrasts. J. Volcanol. Geotherm. Res., 333, 96-103.

Rahimi, H., H. Hamzehloo (2008). Lapse time and frequency-dependent attenuation of coda waves in the Zagros continental collision zone in Southwestern Iran, J. Geophys. Eng., 5, 173-185.

Rahimi, H., K. Motaghi, S. Mukhopadhyay, H. Hamzehloo (2010). Variation of coda wave attenuation in the Alborz region and central Iran, Geophys. J. Int., 181, 1643-1654.

Ranasinghe, N. R., A. C. Gallegos, A. R. Trujillo, A. R. Blanchette, E. A. Sandvol, J. Ni, T. M. Hearn, Y. Tang, S. P. Grand, F. Niu, Y. J. Chen, J. Ning, H. Kawakatsu, S. Tanaka, M. Obayashi (2014). Lg attenuation in northeast China using NECESSArray data, Geophys. J. Int., 200(1), 67-76.

Rautian G., I. Khalturin (1978). The use of the coda for determination of the earthquake source spectrum, Bull. Seis. Soc. Am., 680, 923-948.

Reilinger, R. E, S. C. McClusky, M. B. Oral, R. W. King, M. N. Toksoz, A. A. Barka, I. Kinik, O. Lenk, I. Sanli (1997). Global Positioning System measurements of present-day crustal movements in the Arabia-Africa-Eurasia plate collision zone, J. Geophys. Res.: Solid Earth, 102, 9983-9999.

Reilinger, R., S. McClusky, P. Vernant, S. Lawrence, S. Ergintav, R. Cakmak, H. Ozener, F. Kadirov, I. Guliev, R. Stepanyan, M. Nadariya, G. Hahubia, S. Mahmoud, K. Sakr, A. ArRajehi, D. Paradissis, A. Al-Aydrus, M. Prilepin, T. Guseva, E. Evren, A. Dmitrotsa, S. V. Flikov, F. Gomez, R. Al-Ghazzi (2006). GPS constraints on continental deformation in the Africa-Arabia-Eurasia continental collision zone and implications for the dynamics of plate interactions, J. Geophys. Res.: Solid Earth, 111, 9983-9999.

Sato, H., M. Fehler (1998). Seismic Wave Propagation and Scattering in the heterogeneous Earth, AIP Press/Springer Verlag, New York, 308 pp.

Sato, H., I. S. Sacks (1989). Anelasticity and thermal structure of the oceanic upper mantle: Temperature calibration with heat flow data, J. Geophys. Res.: Solid Earth, 94.B5, 5705-5715.

Sertcelik, F., M. Guleroglu (2017). Coda Wave Attenuation Characteristics for North Anatolian Fault Zone, Turkey, Open Geosci., 9(1), 480-490.

Sertçelik, F. (2012). Estimation of coda wave attenuation in the east Anatolia fault zone, Turkey. Pure Appl. Geophys., 169(7), 1189-1204.

Sharma, B., D. Kumar, S. S. Teotia, B. K. Rastogi, A. K. Gupta, S. Prajapati (2012). Attenuation of Coda Waves in the Saurashtra Region, Gujarat (India), Pure Appl. Geophys., 169, 89-100.

Singh, C., A. Singh, V. K. S. Bharathi, A. R. Bansal, R. K. Chadha (2012). Frequency-dependent body wave attenuation characteristics in the Kumaun Himalaya, Tectonophysics, 524, 37-42.

Spudich, P., T. Bostwick (1987). Studies of the seismic coda using an earthquake cluster as a deeply buried seismograph array, J. Geophys. Res., 92(B10), 10526-10546.

Stein, S., M. Wysession (2009). An introduction to seismology, earthquakes, and earth structure. John Wiley & Sons.

Tunç, B., D. Çaka, T. S. Irmak, H. Woith, S. Tunç, . Barı , M. F. Özer, B. G. Lühr, E. Günther, H. Grosser, J. Zschau (2011). The Armutlu Network: an investigation into the seismotectonic setting of Armutlu–Yalova–Gemlik and the surrounding regions. Ann. Geophys., 54, 35-45.

Yavuz, E., D. Çaka, B. Tunç, T. S. Irmak, H. Woith, S. Cesca, B. G. Lühr, Ş. Barış (2015). Earthquake Swarm

in Armutlu Peninsula, Eastern Marmara Region, Turkey, EGU General Assembly Conference Abstracts. 17.

Yavuz, E., D. Çaka, B. Tunç, H. Woith, B. G. Lühr, Ş. Barış (2016). Attenuation Characteristics of the Armutlu Peninsula (NW Turkey) Using Coda Q, EGU General Assembly Conference Abstracts. 18.

Yilmaz, Y., Ş. C. Genç, E. Yiğitbaş, M. Bozcu, K. Yılmaz (1995). Geological evolution of the late Mesozoic continental margin of Northwestern Anatolia, Tectonophysics, 243, 155-171.

*CORRESPONDING AUTHOR: Evrim YAVUZ,
Kocaeli University, Dept. of Geophysical Engineering,
Umuttepe, 41380 Kocaeli, Turkey
email: evrim.yavuz@kocaeli.edu.tr